Korean J. Chem. Eng., 38(2), 366-379 (2021)
DOI: 10.1007/s11814-020-0697-9

pISSN: 0256-1115
eISSN: 1975-7220

Mathematical and experimental modeling of reverse osmosis (RO) process

Zeinab Hadadian*,†, Sina Zahmatkesh*, Mostafa Ansari*, Ali Haghighi*, and Eskandar Moghimipour**

*Faculty of Civil Engineering and Architecture, Shahid Chamran University of Ahvaz, Ahvaz, Iran
**Nanotechnology Research Center, Ahvaz Jundishapur University of Medical Sciences, Ahvaz, Iran
(*Received 13 May 2020 • Revised 26 September 2020 • Accepted 15 October 2020*)

Abstract−This paper provides a mathematical simulation model for the reverse osmosis (RO) process with series elements. A mathematical simulation model was developed based on the mass, material and energy balances considering the concentration polarization. The simulation model is open-source and easy to couple with other computational tools like optimization algorithms and SCADA[1] applications. An RO laboratory pilot was also set up in the Hydraulic Lab of Shahid Chamran University of Ahvaz to validate the simulation results. Comparing the results of the simulation model with the experiments and ROSA commercial software, the proposed simulation model functions well and is reliable. The comparisons indicate that the simulation results are over 96% close to ROSA and over 80% close to experimental results.

Keywords: Desalination, Reverse Osmosis, Simulation, Experimental, Mathematical Modeling

INTRODUCTION

The reverse osmosis (RO) method for desalination is currently the most popular technology for seawater and brackish water desalination [1]. The RO process has several advantages over the other desalination methods, especially in terms of energy consumption and efficiency. For each RO system, the membrane performance should be evaluated to determine the type of membrane, recovery, and number of membrane elements. The construction and operation costs, as well as the permeate concentration and the permeate flux, are critical factors to determine for the design of an RO system. Commercial software, like ROSA and IMSDesign, has been widely used in many investigations and industrial projects for predicting the performance of the RO systems [2]. These commercial models have been mostly released by the membrane manufacturers and therefore are useful for their productions. For research objectives, one needs to have an open-source model to extend the simulations and couple the RO models with the optimization algorithms and other mathematical techniques.

Villafafila and Mujtaba developed a simulation and optimization model for seawater and brackish water. They optimized energy consumption, recovery, and the number of tubular membranes. They considered the number of pressure vessels, pressure values, membrane diameter, and feed water flux as the constraints [3]. Barello et al. provided experimental data that examined the pure water permeability and salt permeability constant for this type of membrane element (tubular) [4]. Marcovecchio et al. optimized the simulation of seawater reverse osmosis (SWRO) system with a two-stage arrangement. That work included hollow fiber membranes and energy recovery systems [5]. Geraldes et al. optimized the simulation of a two-stage desalination system and the considered spiral wound membrane (the most common type). They also used the experimental data to identify specific parameters in design equations. That paper focused on optimizing the pressure and flow of feed water for various recovery rates [6]. Guria et al. presented a multiobjective optimization problem for seawater desalination, using spiral wound and tubular membranes. That paper does not include experimental data [7]. An optimization model for different feed water concentrations was presented by Lu et al. in 2007 [8]. Choi et al. presented an RO and forward osmosis (FO) computer program; the model was developed only for a one-stage system [9]. Du et al. presented a simulation-optimization model for seawater and brackish water, using spiral wound membranes. They considered the permeate flux as a constraint in addition to the constraints on the membrane manufacturer. The model also included a maximum of two-stage membrane and considered energy recovery systems [10-12]. Altaee estimated the performance of RO systems with several elements based on the solution-diffusion model, and most of the equations used in that paper were from the empirical equations presented in the DOW design guide, which included single-stage systems and has no experimental data. It was a model that was unable to establish new constraints or to optimize the system [2]. Saavedra et al. presented a design method for RO brackish water plants, which was based on the application of maximum available recovery without scaling of any inorganic compounds presented in water [13,14]. Choi and Kim presented a simulation and optimization model for RO systems with two stages, including spiral wound membranes, but did not provide experimental work [15]. Kotb et al. examined an SWRO system with a maximum of three-stages [16]. Haluch et al. evaluated the experimental and semi-empirical model of a small-capacity reverse osmosis desalination unit. They found that the semi-empirical model predictions agreed with their experimental counterparts within the measurement uncertainty threshold [17]. Chee et al. investigated the performance evaluation

[1]Supervisory Control And Data Acquisition

†To whom correspondence should be addressed.
E-mail: z-hadadian@phdstu.scu.ac.ir

of RO desalination pilot plants using the ROSA Simulation software. They found that in terms of flux and recovery ratio, the simulated results and the experimental data showed a marginal discrepancy with deviations <2% and <8%, respectively. Their findings also confirmed the feasibility of adopting ROSA software to verify the performance of a pilot plant with all operational parameters being ideally optimized [18]. Al-Obaidi et al. evaluated the performance of a medium-sized industrial BWRO desalination plant of the Arab Potash Company using the mathematical model and the real data [19]. Chen and Qin developed mathematical modeling of glucose-water separation through reverse osmosis (RO) membrane to research the membrane's performance during the mass transfer process. They validated the model using experimental results and found that the calculated results were consistent with the experimental data [20]. Maure and Mungkasi obtained a mathematical model using numerical integration for the reverse osmosis system [21]. Li proposed a predictive mathematical model based on the solution-diffusion theory for a commercial spiral wound SWRO module. They concluded that the mathematical model with the parameters obtained from the experimental data can predict the flow of water and salt as well as the pressures under different feed conditions of temperature, flow, and pressure with a mean error ≤4% [22]. Gaublomme et al. developed a generic steady-state model for RO and applied it to a unique three-year data set of a full-scale RO process. They validated the model with online conductivity data as input taking into account the uncertainty originating from online sensors and compared to the commercial software Winflows. They found that the model has satisfactory results, i.e., an average deviation from the data at 2.7%, 12.7%, 34.1% and 18.7%, respectively, for the recovery, the concentrate pressure, the permeate, and concentrate solute concentration [23]. Siegel et al. developed a mathematical model describing the RO enrichment process using a novel device. They created it in MATLAB Simulink software and validated it with experimental results. Using the calculation of the mean relative error between the model and the experimental results, they concluded that the model is useful for describing the RO system and the RO device is suitable for the enrichment of estrogens prior to instrumental or in vitro analysis [24]. Ligaray et al. presented a novel energy self-sufficient desalination system design that incorporates rechargeable seawater batteries as an additional energy storage system. They predicted the experimental data using the ROSA model to determine the configuration of the lowest energy consumption and highest charging rate. The results showed that the seawater battery achieved satisfactory desalination performance [25]. Mansour et al. focused on employing an energy recovery system (ERS) to enhance the performance of the small RO plant for remote areas using an experimental pilot and simulation model. Their obtained results showed good agreement between experimental and simulation model values. They evaluated the cost analysis of the small RO desalination plant with and without ERS and showed a significant reduction in total cost [26].

In this paper, we present a mathematical simulation program for a multi-element RO system and consider multiple elements in each pressure vessel. The output parameters of the program include the feed pressure, the permeate concentration, the recovery of each element in the pressure vessel, and the permeate flow generated by each element. Unlike other commercial software (ROSA, IMSDesign, etc.), the proposed model is open-source and easy to couple with other computational tools like optimization algorithms, and since it has been based on the mathematical equations of the RO process (the ROSA software utilizes experimental equations that control Filmtec membranes), it is capable of using all types of membranes manufactured in different companies. In existing commercial software, the total system recovery is considered as input, while the present model considers the recovery of each stage separately. An RO laboratory pilot with 50 m^3/day production capacity has been also set up in the Hydraulic Lab of Shahid Chamran University of Ahwaz to validate the simulation results. Two single-element and multi-element cases were simulated using the proposed simulator model and the results were compared with the ROSA software simulation and the experimental results which are discussed.

MATERIALS AND METHODS

1. Model Development

An RO mathematical simulation model was developed based on mass, material, and energy balances for a given configuration. For more realistic modeling, the concentration polarization is also taken into account. The related equations used to simulate the RO process are reported in Table 1.

2. Membrane Characteristics

The full characteristics of the membranes provided by the manufacturers are critical parameters for the simulation of the RO systems. The required data include the active membrane area, maximum operating pressure, salt rejection, pure water permeability constant (A_m), feed spacer, pressure drop in element, length of the element, diameter of the element, spacer diameter and thickness.

3. Arrangements of a Multi-stage RO System

The schematic of a multi-stage RO unit is shown in Fig. 1.

For a three-stage system, there are three splitter points (F, R1, and R2) with three split ratios α, β and γ between 0 and 1 so that their summation at each point is 1. The flow rate of the feed solution to each stage can be calculated by Eq. (16) [16].

$$\begin{cases} Q_{f1} = \alpha_f Q_f \\ Q_{f2} = \gamma_f Q_f + \gamma_{R1} Q_{R1} \\ Q_{f3} = \beta_f Q_f + \beta_{R1} Q_{R1} + \beta_{R2} Q_{R2} \end{cases} \tag{16}$$

where, Q_{R1} is retentate flow rate from the first stage (m^3/s), Q_{R2} is retentate flow rate from the second stage (m^3/s), Q_{F1} is feed flow rate to the first stage (m^3/s), Q_{F2} is feed flow rate to the second stage (m^3/s), Q_{F3} is feed flow rate to the third stage (m^3/s), α is the fraction of stream branching to the left from a split point, β is the fraction of stream branching to the right from a split point, and γ is the fraction of stream branching straight forward from a split point.

4. The Calculation of Permeate Water at Each Stage

The purpose of the RO simulation is to determine the pressure required at each stage to obtain the required permeate water. Each stage may include several pressure vessels in parallel, and each pressure vessel includes several membranes in a series. The number of pressure vessels in each stage depends on the total number of the

Table 1. Equations for the RO process simulation

Meaning	Equation	No.	Ref.
Feed flow rate	$Q_F = Q_R + Q_P$	(1)	[1]
Permeate flow rate	$Q_P = TCF(j_w A)$	(2)	[1]
Temperature correction factor	$TCF = \begin{cases} 1, & T_F = 25\ ^{\circ}C \\ \exp\left(\frac{25{,}000}{R}\left(\frac{1}{T_0+273.15} - \frac{1}{T_F+273.15}\right)\right), & T_F > 25\ ^{\circ}C \\ \exp\left(\frac{20{,}000}{R}\left(\frac{1}{T_0+273.15} - \frac{1}{T_F+273.15}\right)\right), & T_F < 25\ ^{\circ}C \end{cases}$	(3)	[10]
Material balance	$Q_F \times C_F = (Q_P \times C_P) + (Q_R \times C_R)$	(4)	[1]
Feed concentration	$C_F = C_P/(1 - \text{rejection})$	(5)	[2]
Permeate water flux	$j_w = A_m(\Delta P - \Delta\pi) = A_m P_{eff}$	(6)	[1]
Residual transmembrane pressure	$P_{eff} = (P_f - P_p - \Delta P_{in} - \Delta P_f/2) - (\pi_w - \pi_p)$	(7)	[1]
Van't hoff's equation	$\pi = nMR(T+273.15)10^{-3}$ For NaCl $\pi = (2(C/0.0585)R(T+273.15))10^{-3}$	(8)	[2]
Concentration on the feed side membrane wall	$\frac{C_w - C_p}{C_f - C_p} = \exp\left(\frac{J_w d}{D_S}\right) = \exp\left(\frac{J_w}{k}\right)$ $C_w = C_P + (C_f - C_p)\exp(J_w/k)$	(9)	[1]
Mass transfer coefficient	$k = 0.5510(Re)^{0.4}(Sc)^{0.17}(C_f/\rho)^{-0.77}(D_S/d)^{-0.77}$	(10)	[9]
Density	$\rho = 498.4m + \sqrt{248{,}400m^2 + 752.4mC_f}$ $m = 1.0069 - 2.757 \times 10^{-4} T_f$	(11)	[1]
Viscosity	$\mu = 1.234 \times 10^{-6} \exp(0.00212C_f + 1{,}965/T_f + 273.15)$	(12)	[1]
Diffusivity	$D_S = 6.725 \times 10^{-6} \exp(0.1546 \times 10^{-3} C_f - 2{,}513/T_f + 273.15)$	(13)	[1]
Effective membrane area	$A_{eff} = (V_T/l) * \varepsilon$ $\varepsilon = 1 - V_{SP}/V_T$	(14)	[23]
Number of pressure vessels in the i^{th} stage	$N_{PVi} = \frac{N_i}{N_{ei}}$	(15)	

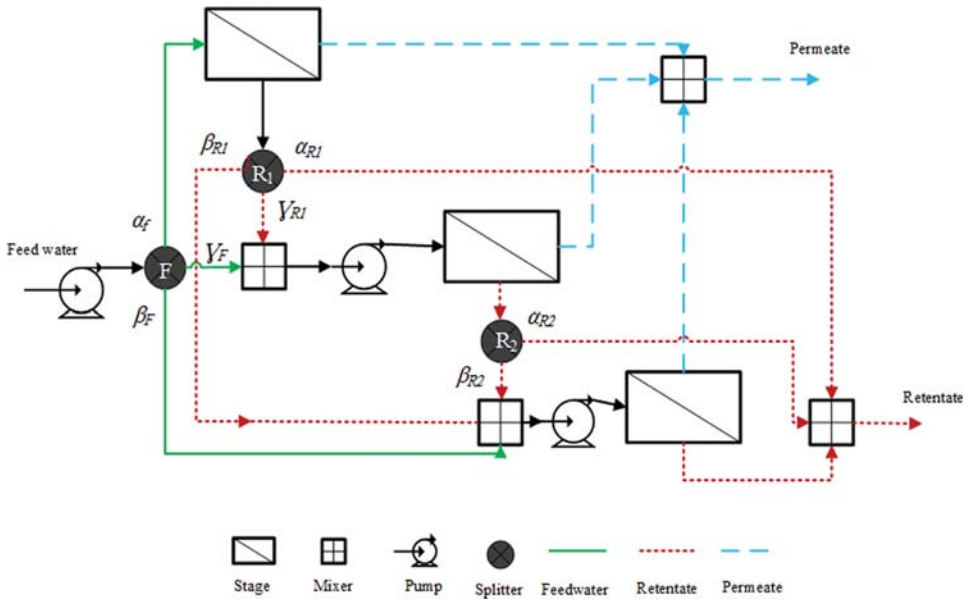

Fig. 1. Schematic of multi-stage RO unit [16].

membranes and the number of membranes in each pressure vessel, which is obtained from Eq. (15). The system recovery depends on the permeate water (Q_p) and the feed flow (Q_f) as follows:

$$\text{Recovery} = \frac{Q_p}{Q_f} \tag{17}$$

Since the amount of permeate water should be constant, by determining the system recovery the amount of feed flow is determined. If we assume the recovery in the first, second, and third stages, respectively, rec1, rec2, and rec3, the amount of permeate water at each stage can be calculated according to Eq. (16) as follows:

$$Q_{f1} = \alpha_f Q_f \Rightarrow Q_f = \frac{Q_{f1}}{\alpha_f}$$

$$Q_{f2} = \gamma_{R1} Q_{R1} + \gamma_f Q_f \xrightarrow{Q_f = \frac{Q_{f1}}{\alpha_f},\ Q_{R1} = (1-rec1)Q_{f1}}$$

$$Q_{f2} = Q_{f1}\left((1-\text{rec1})\gamma_{R1} + \frac{\gamma_f}{\alpha_f}\right) \tag{18}$$

$$\xrightarrow{Q_f = \frac{Q_p}{rec}} \frac{Q_p}{\text{rec2}} = \frac{Q_{p1}}{\text{rec1}}\left((1-\text{rec1})\gamma_{R1} + \frac{\gamma_f}{\alpha_f}\right)$$

$$Q_{f3} = \beta_{R2} Q_{R2} + \beta_f Q_f + \beta_{R1} Q_{R1}$$

$$= \beta_{R2}(1-\text{rec2})Q_{f2} + \beta_{R1}(1-\text{rec1})Q_{f1} + \frac{\beta_f}{\alpha_f} Q_{f1} \tag{19}$$

$$\frac{Q_{p3}}{\text{rec3}} = \frac{\beta_{R2}(1-\text{rec2})}{\text{rec2}} Q_{p2} + \left(\frac{\beta_{R1}(1-\text{rec1})}{\text{rec1}} + \frac{\beta_f}{\alpha_f \text{rec1}}\right) Q_{p1}$$

By using Eqs. (18) and (19) along with the continuity equation, the values of productive permeate water are obtained at each stage as follows:

$$\begin{cases} \dfrac{(1-\text{rec1})\gamma_{R1} + \dfrac{\gamma_f}{\alpha_f}}{\text{rec1}} Q_{p1} - \dfrac{Q_{p2}}{\text{rec2}} = 0 \\ \left(\dfrac{\beta_{R1}(1-\text{rec1})}{\text{rec1}} + \dfrac{\beta_f}{\alpha_f \text{rec1}}\right) Q_{p1} + \dfrac{\beta_{R2}(1-\text{rec2})}{\text{rec2}} Q_{p2} - \dfrac{Q_{p3}}{\text{rec3}} = 0 \\ \sum_{i=1}^{3} Q_i = Q_p \end{cases} \tag{20}$$

Finally, the feed rate intake at each stage can be determined by having Q_{p1}, Q_{p2}, Q_{p3}, the recovery, and the coefficients of the splitter points.

5. The Calculation of Operating Parameters for Each Element of Pressure Vessel

Given that there is uniformity of the pressure vessels at each stage, the feed flow and permeate flow rates are split equally among the pressure vessels and are obtained for each pressure vessel (QF_{PVj}, QP_{PVj}). In each pressure vessel permeate water produced by the elements is calculated using Eqs. (2), (6), and (7) as in the following equation:

$$Q_{Pz} = A * TCF * A_m\left(\left(P_f - P_{pz} - \Delta P_{inz} - \frac{\Delta P_{fz}}{2}\right) - (\pi_{wz} - \pi_{pz})\right) \tag{21}$$

By placing Eqs. (8), (9), and (5) in Eq. (21):

$$Q_{Pz} = A * TCF * A_m\left(\left(P_f - P_{pz} - \Delta P_{inz} - \frac{\Delta P_{fz}}{2}\right) - \left(\frac{2R(T+273.15)}{0.0585} * 10^{-3}\right)(C_{wz} - C_{Pz})\right)$$

$$Q_{Pz} = A * TCF * A_m\left(\left(P_f - P_{pz} - \Delta P_{inz} - \frac{\Delta P_{fz}}{2}\right) - \left(\frac{2R(T+273.15)}{0.0585} * 10^{-3}\right)\left(C_{Pz} + (C_{fz} - C_{pz})\exp\left(\frac{J_w}{k_z}\right) - C_{Pz}\right)\right) \tag{22}$$

$$Q_{Pz} = A * TCF * A_m\left(\left(P_f - P_{pz} - \Delta P_{inz} - \frac{\Delta P_{fz}}{2}\right) - \left(\frac{2R(T+273.15)}{0.0585} * 10^{-3}\right) * C_{Pz}\left(\frac{1}{1-\text{rejection}} - 1\right) * \exp\left(\frac{Q_{Pz}}{A * k_z}\right)\right)$$

In each pressure vessel, the feed flow rate and feed pressure inlet to each element are equal to the retentate flow rate and retentate pressure outlet from the previous element.

$$Q_{Fz+1} \times C_{Fz+1} = Q_{Fz} \times C_{Fz} - Q_{Pz} \times C_{Pz} \tag{23}$$

$$Q_{Fz+1} = Q_{Fz} - Q_{Pz} \tag{24}$$

By using Eqs. (5), (23), and (24), the permeate concentration at the z+1th element is obtained as follows:

$$C_{Pz+1} = (1-\text{rejection})\left[\frac{Q_{Fz} \times \dfrac{C_{Pz}}{1-\text{rejection}} - Q_{Pz} \times C_{Pz}}{Q_{Fz} - Q_{Pz}}\right] \tag{25}$$

For each pressure vessel, the summation of permeate flux of all elements is equal to the required permeate flux of the pressure vessel.

$$Q_{Ppvj} = \sum_{z=1}^{Nei} Q_{Pz} \tag{26}$$

Then, for all elements in the pressure vessel, a set of nonlinear equations consisting of permeate flow rate (Eq. (22)) and concentration (Eq. (25)) as variables with Eq. (26) is formed, which is solved by the Newton-Raphson method and obtained feed water pressure of that stage and permeate flow rate and concentration in each element.

Finally, the permeate concentration of the jth pressure vessel (Cp_{pvj}) is calculated as follows:

$$C_{Ppvj} = \frac{\sum_{z=1}^{Nei}(Q_{Pz} * C_{Pz})}{Q_{Ppvj}} \tag{27}$$

Total permeate concentration and recovery of the system are calculated as follows:

$$Cp_{total} = \frac{\sum_{i=1}^{3}(Q_{Pi} * C_{Pi})}{Q_P} \tag{28}$$

$$\text{rec}_{total} = \frac{Q_P}{Q_f} = \frac{Q_P}{Q_{f1}/\alpha_f} = \frac{Q_P}{Q_{p1}/(\text{rec1} * \alpha_f)} \tag{29}$$

6. The Simulation Algorithm

The solving procedure of the RO equations is illustrated in Fig. 2. The simulation model is mathematically nonlinear and implicit and should be iteratively solved. The proposed simulation algorithm consists of the following steps:

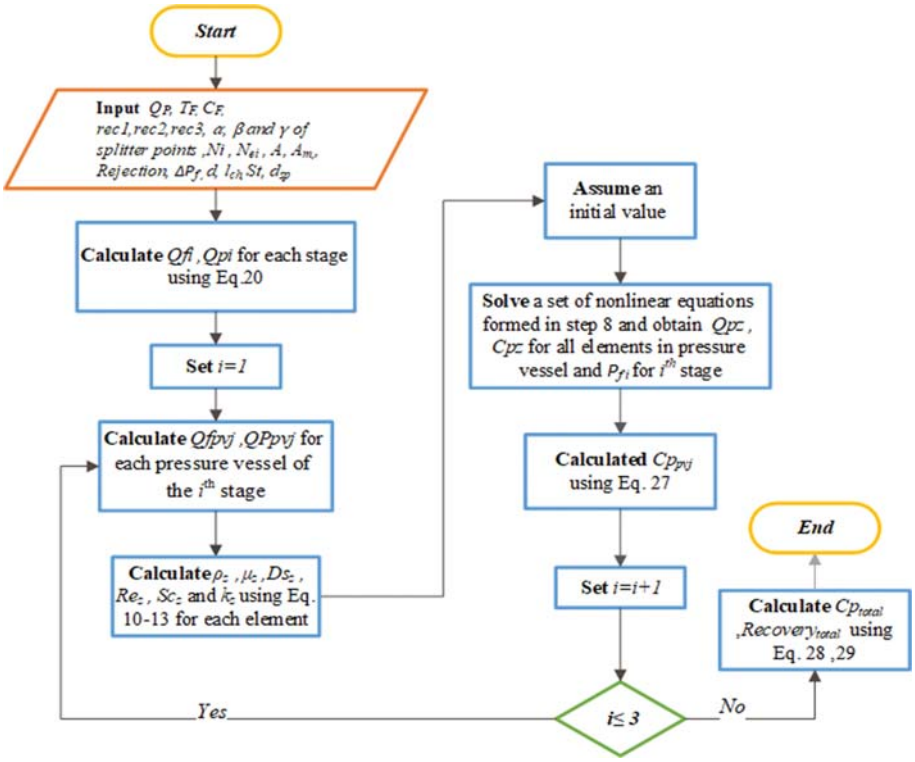

Fig. 2. Flowchart of RO simulation model.

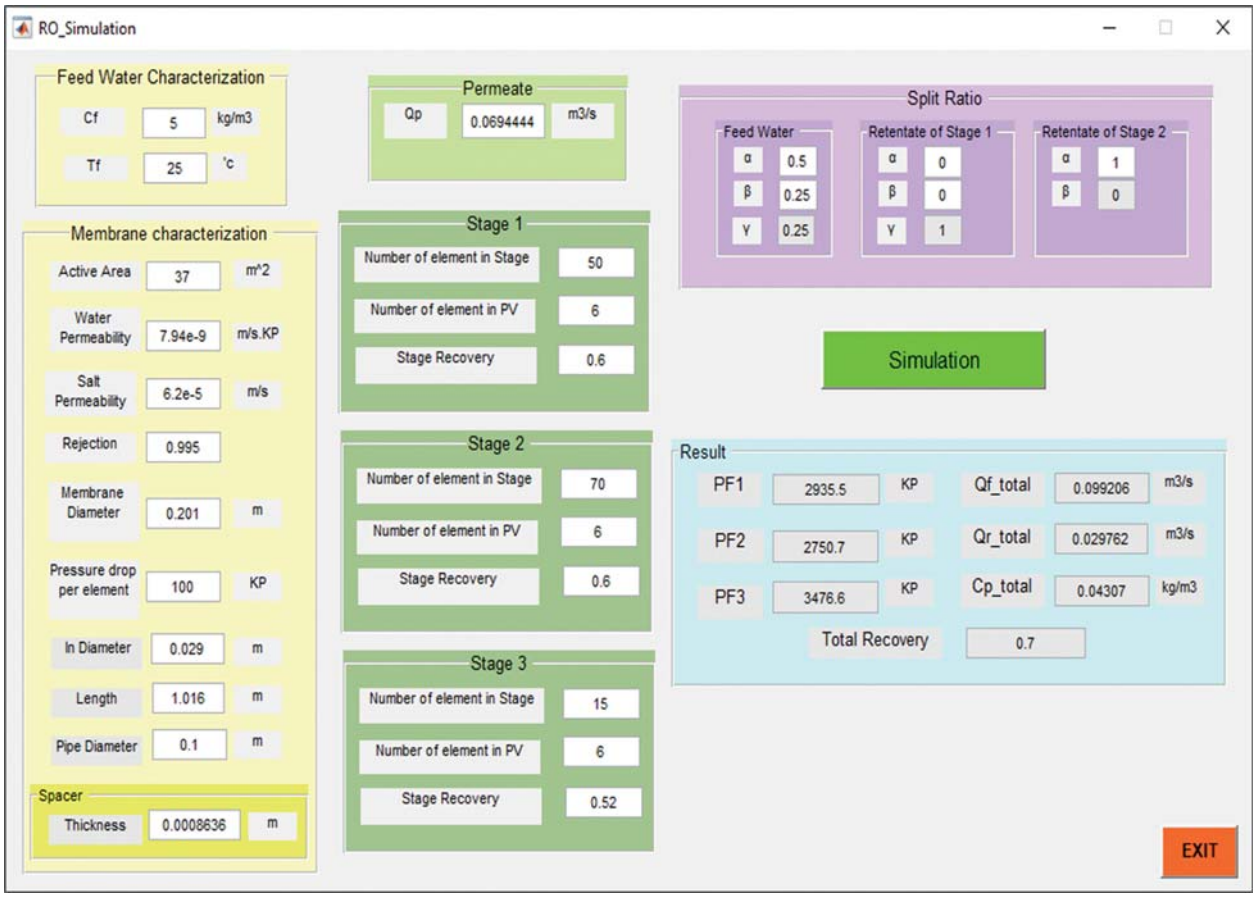

Fig. 3. A graphical user interface (GUI) window.

1. The input data include the feed water and membrane characteristics, recovery of each stage, required permeate water, number of elements, the number of series element in each pressure vessel, and the split ratios for the membrane's arrangement are introduced to the model.

2. Q_{Pi} is calculated using Eq. (20) for each stage (i=1 : 3) then Q_{Fi} and Q_{Ri} are obtained using Eqs. (17) and (1), respectively.

3. Set i=1 for the first stage

4. QF_{PVj}, QP_{PVj} are calculated for each pressure vessel (j=1: N_{PVi}) in i^{th} stage and because of the uniformity of the pressure vessels at each stage, Q_{Fi} and Q_{Pi} are split equally among the pressure vessels.

5. ρ_z, μ_z, Ds_z, Re_z, Sc_z, and k_z are calculated using Eqs. (10)-(13) for each element.

6. Each pressure vessel assumes an initial value for the feed water pressure (P_{Fi}) and permeate flow rate, and concentration in each element (z=1: N_{ei}).

7. Due to the similarity of the pressure vessels in a stage, the pressure in all pressure vessels is equal to the pressure applied by the pump to the stage. The input pressure to the first element has been already assumed in step 6.

8. Solving Eqs. (22), (25), and (26) for all elements (z=1: N_{ei}) in a pressure vessel in a set of nonlinear equations, which is solved by the Newton-Raphson method.

9. Permeate concentration of pressure vessel (Cp_{pvj}) is calculated using Eq. (27).

10. Steps 4 to 9 are repeated for all stages.

Based on the above algorithm, simulation software with a graphical user interface (GUI) was designed in MATLAB. This algorithm makes it possible to do the RO simulation by entering the initial data, feed water, and membrane characteristics to obtain the required feed pressures for stages, feed flow rate, retentate flow rate, and the permeate concentration as displayed in Fig. 3.

EXPERIMENTAL

1. Experimental Pilot

An RO experimental pilot with 50 m^3/day production capacity was constructed at the Hydraulic Lab of Shahid Chamran University of Ahwaz and used to validate the results of this simulation model. This pilot is shown in Figs. 4-5 and includes both pretreatment and desalination units. The pretreatment unit consists of a booster pump (1.34 kW), a carbon filter, a sand filter, four micro-filters (5 microns), and a water tanker. The desalination unit consists of a water tanker with a mixer, a booster pump (1.21 kW), a high-pressure pump (3.06 kW), and a BW30-400 membrane from DOW. The membrane's characteristics are given in Table 2. The pressure and flow through

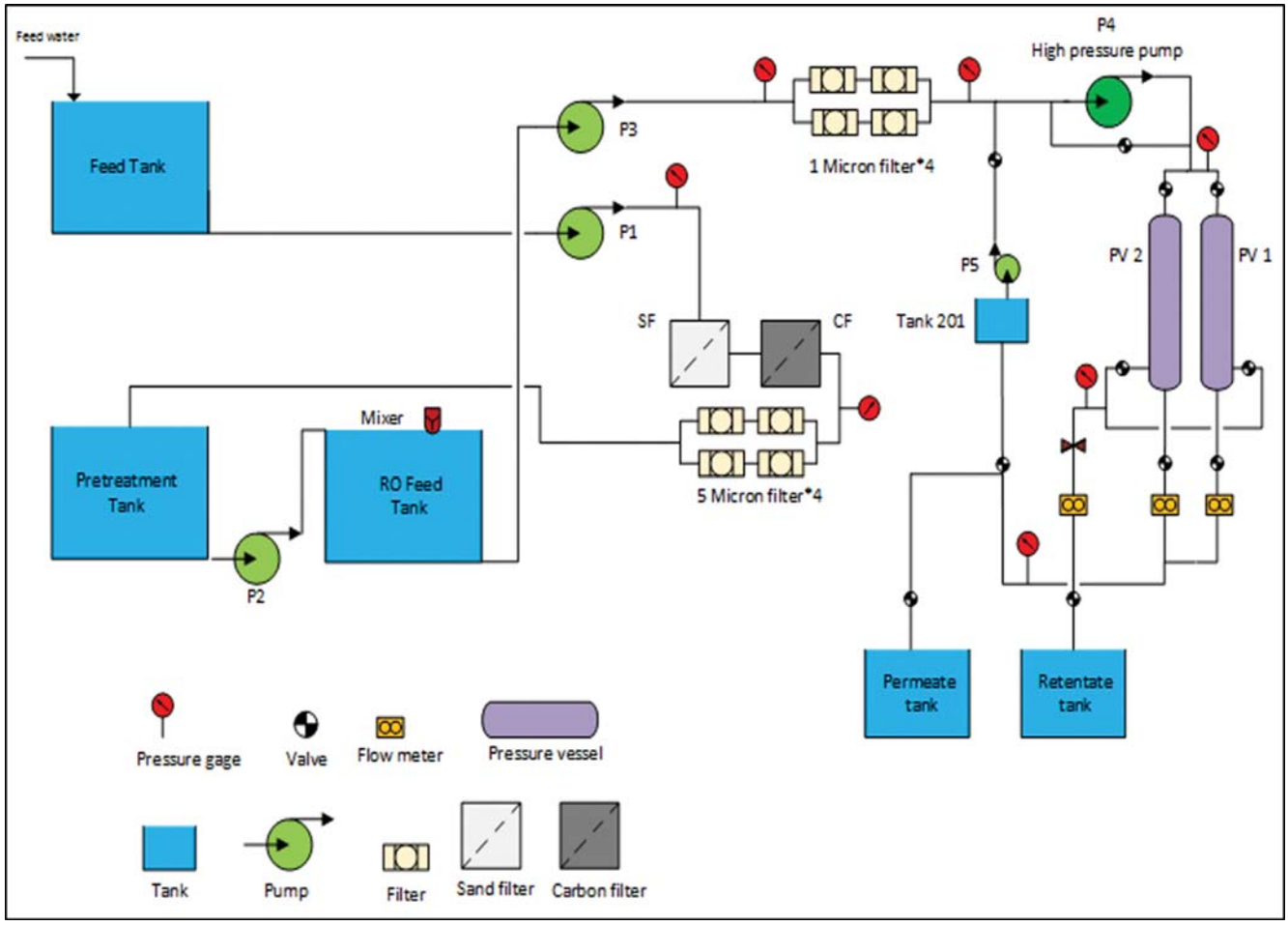

Fig. 4. Flowchart of the RO pilot plant at Hydraulic Lab of Shahid Chamran University of Ahvaz.

Fig. 5. The RO pilot plant at Hydraulic Lab of Shahid Chamran University of Ahvaz.

the process are also measured by pressure gauges and flow meters in different parts in the system. The value of pure water permeability constant for the BW30-400 membrane was found 7.94e-9 (m/s·kPa) through experimental data analysis and calibration.

2. Test Cases and Methodology of the Experiments

To validate the simulation model, some RO experiments were carried out at the pressures of 700 and 1,100 kPa for the brackish water as feed solution with a concentration of 2-5 kg/m^3 by the RO plant. For all tests feed water temperature was 15 °C and PH=7.3± 0.1. Each RO experiment was performed by maintaining the feed pressures constantly and varying the concentration of the feed solution from 2-5 kg/m^3. The flow rate and concentration of permeate and retentate water were measured, and then the recovery of each case was calculated for the applied pressure.

RESULTS AND DISCUSSION

In this study, a simulator model for the RO process was developed and validated by the ROSA software and an experimental pilot.

1. Performance of the Experimental Pilot

The performance evaluation of the laboratory scale experiments was conducted with various operating conditions, including operating pressure (700 and 1,100 kPa) and feed concentration (2, 3, 4, 5 kg/m^3). The experimental results are reported in Fig. 6. Our experiments were limited to operating pressures below 1,100 kPa and recovery ratios below 50%.

As shown in Fig. 6(a), at constant pressure, the increase of the feed concentration from 2 to 5 kg/m^3 decreases the permeate flow rate from 9.55 to 3.75 (m^3/min)*10^{-3} and 15.29 to 10.55 (m^3/min)*10^{-3} for experimental pressure of 700 and 1,100 kPa, respectively. In addition, the decreasing trend was almost linear with correlation coefficients of 0.9888 and 0.9961 for experimental pressures of 700 and 1,100 kPa, respectively. The highest permeate flow rate (15.29 (m^3/min)*10^{-3}) was obtained at pressures of 1,100 kPa and feed concentration of 2 kg/m^3. A higher permeate flow rate means that the membrane can produce a large amount of water per unit area and time. At a constant feed concentration, with increasing pressure from 700 to 1,100 kPa, the permeate flow rate also increases by 5.74, 5.42, 6.64, and 6.8 (m^3/min)*10^{-3}) at feed concentration of 2, 3, 4, and 5, respectively. This is an acceptable issue and can be justified using Eq. (6). According to this equation at constant pressure, the permeate flow rate decreases with increasing osmotic pressure due to increasing feed concentration. At a constant feed concentration, the permeate flow rate also increases when increasing the pressure.

Fig. 6(b) indicates that the highest recovery was obtained by 48.58% at pressure of 1,100 kPa and feed concentration of 2 kg/m^3. As shown in this figure, at constant pressure, the increase of the feed concentration from 2 to 5 kg/m^3 decreases the recovery from 41.54% to 20.67% and 48.58% to 37.06% for experimental pressure of 700 and 1,100 kPa, respectively. At a constant feed concentration, with increasing pressure from 700 to 1,100 kPa, the recovery also increases by 7.04%, 7.05%, 12.9%, and 16.39% at feed concentrations of 2, 3, 4, and 5, respectively, and the average percentage of increased recovery was 10.85%. In other words, the higher the concentration is the higher the percent recovery.

As shown in Fig. 6(c), at constant pressure, the increase in the feed concentration from 2 to 5 kg/m^3 decreases the salt rejection from 96.6% to 94.58% and 97.45% to 96.52% for experimental pressure of 700 and 1,100 kPa, respectively. The salt rejection also increases by increasing the feed pressure at a constant feed concentration. It can also be justified using Eq. (5). The highest salt rejection was obtained at 97.45% at pressures of 1,100 kPa and feed concentration of 2 kg/m^3 and the average salt rejection was 96.36%.

Since energy consumption is a key factor that affects the cost of the RO system, the change of the specific energy consumption (SEC) values versus the feed concentration for experimental pressure of 700 and 1,100 kPa is shown in Fig. 6(d). The SEC is directly related

Table 2. Characteristics of Filmtec spiral wound RO membrane element [27]

Element type	Size (m)	Active surface area (m^2)	Feed spacer thickness (mil)	Applied pressure (kPa)	Salt rejection
BW30-400	0.203*1.02	37.2	28	1,551.32	99.5%

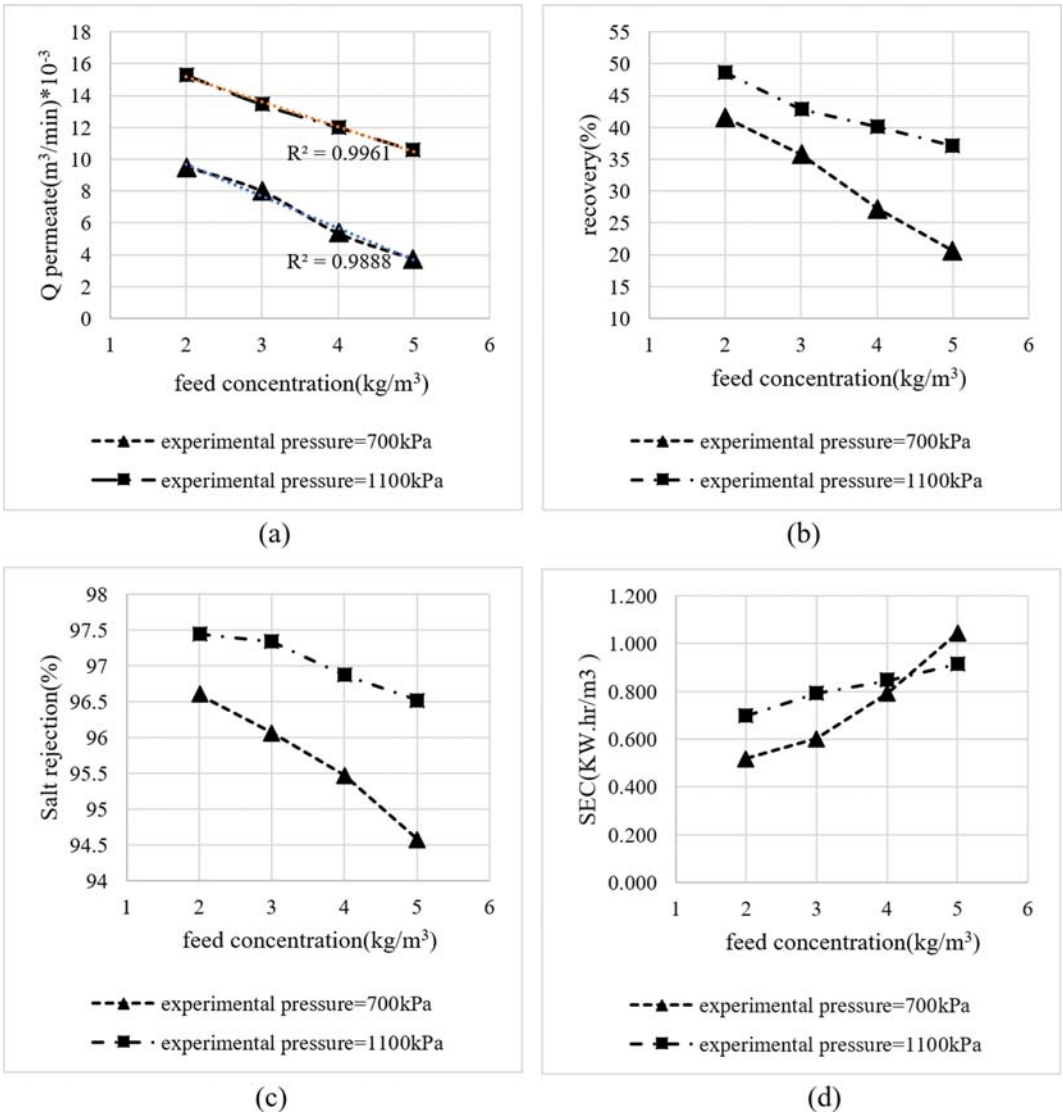

Fig. 6. Experimental result of (a): The permeate flow rate, (b) the recovery of system, (c) the salt rejection, and (d): The specific energy consumption (SEC) versus feed concentration.

to the feed flow rate and pressure (pump power) and inversely related to the permeate flow rate. As shown in this figure, at constant pressure, the increase of the feed concentration from 2 to 5 kg/m^3 increases the SEC. This is because according to Fig. 6(b), the permeate flow rate decreases when increasing the feed concentration and due to increases of SEC. The average SEC value was 0.777 (kW hr/m^3) and all SEC values were less than 1.04 (kW hr/m^3).

2. Performance of the Proposed Simulation Model

2-1. Single Element Case

To validate the simulation model, the RO experiments (Fig. 6) were also simulated by the proposed simulation model as well as by the ROSA software version 9.1. Note that the temperature of the laboratory was rectified using the temperature correction factor TFC in the simulation model equations (Eq. (3)). Tables 3 and 4 compare the results of the RO experimental pilot, the ROSA software estimation, and estimated by the proposed simulator model for the feed concentration of 2, 3, 4, and 5 kg/m^3 and experimental pressure of 700 and 1,100 kPa, respectively. These tables show how, under the same conditions of feed flow rate and recovery, by increasing the feed concentration, the feed pressure decreases in both the ROSA software and simulator models and it can be justified using Eq. (6). The feed pressure estimated by the proposed model is also closer to the estimation by the ROSA software than the experimental. Since the feed pressure has a direct effect on the calculation of energy consumption, this is also true for SEC. The highest SEC values were 1.115 and 1.047 (kW hr/m^3) in the ROSA software and the proposed model, respectively.

To better understand the feed pressure trend, the data sets are shown in Figs. 7 and 8. As shown in Fig. 7, when the experimental pressure was 700 kPa, at the same recovery and the same feed flow rate, by increasing the feed concentration from 2 to 5 kg/m^3, the feed pressure in both the ROSA software and simulator models has a decreasing trend and as shown from 936 to 702 kPa and 896 to 714 kPa in the proposed simulation model and the ROSA

Table 3. Comparison of the results for a single element case (experimental pressure=700 kPa)

	Experimental	ROSA	Proposed model
Feed concentration (kg/m^3)	2	2	2
Q feed (m^3/min)*10^{-3}	22.99	22.99	22.99
Recovery (%)	41.54	41.54	41.54
P feed (kPa)	700	896	936
SEC (kW hr/m^3)	0.52	0.695	0.742
TDS permeate (kg/m^3)	68	20.41	67.3
Salt rejection (%)	96.6	98.98	96.64
Feed concentration (kg/m^3)	3	3	3
Q feed (m^3/min)*10^{-3}	22.39	22.39	22.39
Recovery (%)	35.82	35.82	35.82
P feed (kPa)	700	888	891
SEC (kW hr/m^3)	0.603	0.768	0.794
TDS permeate (kg/m^3)	118	36.89	116.75
Salt rejection (%)	96.07	98.77	96.11
Feed concentration (kg/m^3)	4	4	4
Q feed (m^3/min)*10^{-3}	19.75	19.75	19.75
Recovery (%)	27.24	27.24	27.24
P feed (kPa)	700	768	758
SEC (kW hr/m^3)	0.793	0.859	0.909
TDS permeate (kg/m^3)	181	68	179.12
Salt rejection (%)	95.48	98.3	95.52
Feed concentration (kg/m^3)	5	5	5
Q feed (m^3/min)*10^{-3}	18.12	18.12	18.12
Recovery (%)	20.67	20.67	20.67
P feed (kPa)	700	715	702
SEC (kW hr/m^3)	1.044	1.047	1.108
TDS permeate (kg/m^3)	271	112.09	268.6
Salt rejection (%)	94.58	97.76	94.63

software, respectively. When increasing the feed concentration, the results of the model, ROSA, and the experimental become closer.

To determine the accuracy of the obtained results, the relative error (RE) value of the results relative to each other, which is defined as %RE (A_B)=|(A−B)/B|*100, has been used. The average RE of the model results compared to the experimental results was 17.39%. The highest and lowest errors were 33.71% and 0.28% at the feed concentration of 2 and 5 kg/m^3, respectively. When increasing the feed concentration, the error decreases. The average RE of the experimental results compared to the ROSA results was 13.46%. The highest and lowest errors were 21.8% and 2.09% at the feed concentration of 2 and 5 kg/m^3, respectively. When increasing the feed concentration, the error decreases. The average RE of the model results compared to the ROSA results was 1.94%. The highest and lowest errors were 4.4% and 0.33% at the feed concentration of 2 and 3 kg/m^3, respectively.

Similarly, for the experimental pressure of 1,100 kPa shown in Fig. 8, at the same recovery and the same feed flow rate, by increasing the feed concentration from 2 to 5 kg/m^3, the feed pressure in both the ROSA software and simulator models has a decreasing trend, and as shown from 1,394 to 1,252 kPa and 1,374 to 1,350 kPa in the proposed simulation model and the ROSA software, respectively, and as the result of Fig. 7 shows by increasing the feed concentration, the results of the model, ROSA, and the experimental become closer. The average RE of the model results compared to the experimental results was 19.61%. The highest and lowest errors were 26.72% and 13.81% at the feed concentration of 2 and 5 kg/m^3, respectively. When increasing the feed concentration, the error decreases. The average RE of the experimental results compared to the ROSA results was 19.02%. The highest and lowest errors were 19.94% and 18.51% at the feed concentration of 2 and 5 kg/m^3, respectively. When increasing the feed concentration, the error decreases. The average RE of the model results compared to the ROSA results was 3.89%. The highest and lowest errors were 7.25% and 1.4% at the feed concentration of 5 and 2 kg/m^3, respectively.

As found in Figs. 7 and 8, in the single element case for the feed pressure result, the average RE was 18.50%, 16.24%, and 2.9% for the model compared to the experimental, experimental compared to the ROSA, and model compared to ROSA, respectively. It can be said that the simulation model is well matched with the ROSA results with over 96% accuracy. However, the calculated pressures by the simulation model and ROSA are over 80% accurately close

Table 4. Comparison of the results for a single element case (experimental pressure=1,100 kPa)

	Experimental	ROSA	Proposed model
Feed concentration (kg/m^3)	2	2	2
Q feed (m^3/min)*10^{-3}	31.47	31.47	31.47
Recovery (%)	48.58	48.58	48.58
P feed (kPa)	1100	1374	1394
SEC (kW hr/m^3)	0.699	0.892	0.886
TDS permeate (kg/m^3)	51	15	50.51
Salt rejection (%)	97.45	99.25	97.47
Feed concentration (kg/m^3)	3	3	3
Q feed (m^3/min)*10^{-3}	31.36	31.36	31.36
Recovery (%)	42.87	42.87	42.87
P feed (kPa)	1100	1350	1326
SEC (kW hr/m^3)	0.792	0.992	0.955
TDS permeate (kg/m^3)	80	25.7	79.32
Salt rejection (%)	97.33	99.14	97.36
Feed concentration (kg/m^3)	4	4	4
Q feed (m^3/min)*10^{-3}	29.94	29.94	29.94
Recovery (%)	40.14	40.14	40.14
P feed (kPa)	1100	1359	1291
SEC (kW hr/m^3)	0.846	1.072	0.992
TDS permeate (kg/m^3)	125	38.44	123.62
Salt rejection (%)	96.88	99.04	96.91
Feed concentration (kg/m^3)	5	5	5
Q feed (m^3/min)*10^{-3}	28.47	28.47	28.47
Recovery (%)	37.06	37.06	37.06
P feed (kPa)	1100	1350	1252
SEC (kW hr/m^3)	0.916	1.151	1.043
TDS permeate (kg/m^3)	174	52.17	172.46
Salt rejection (%)	96.52	98.96	96.55

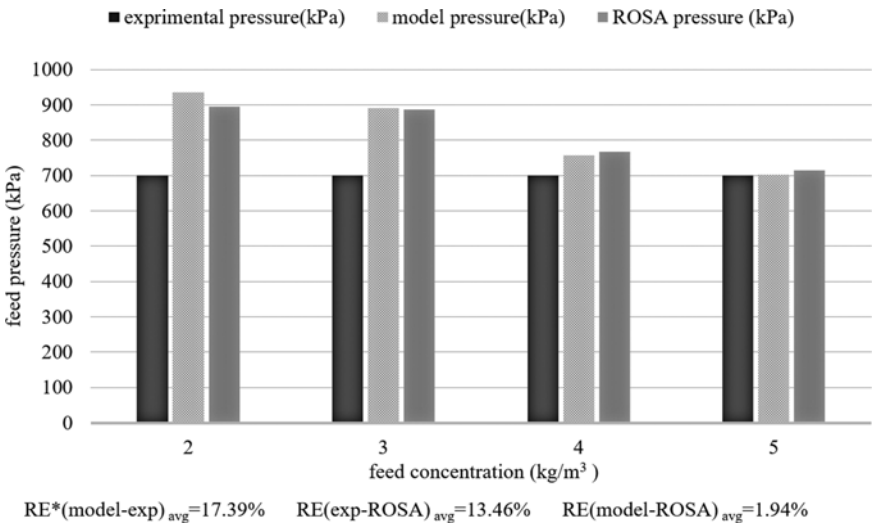

Fig. 7. Variation of feed pressure in RO system with feed concentration (experimental pressure=700 kPa) (*: Relative Error).

to the laboratory results. This could be due to laboratory conditions, measurement errors, and uncertainties and the simplifications applied to the simulation equations. Since the equations used in ROSA and the proposed simulation model are slightly different, this little dif-

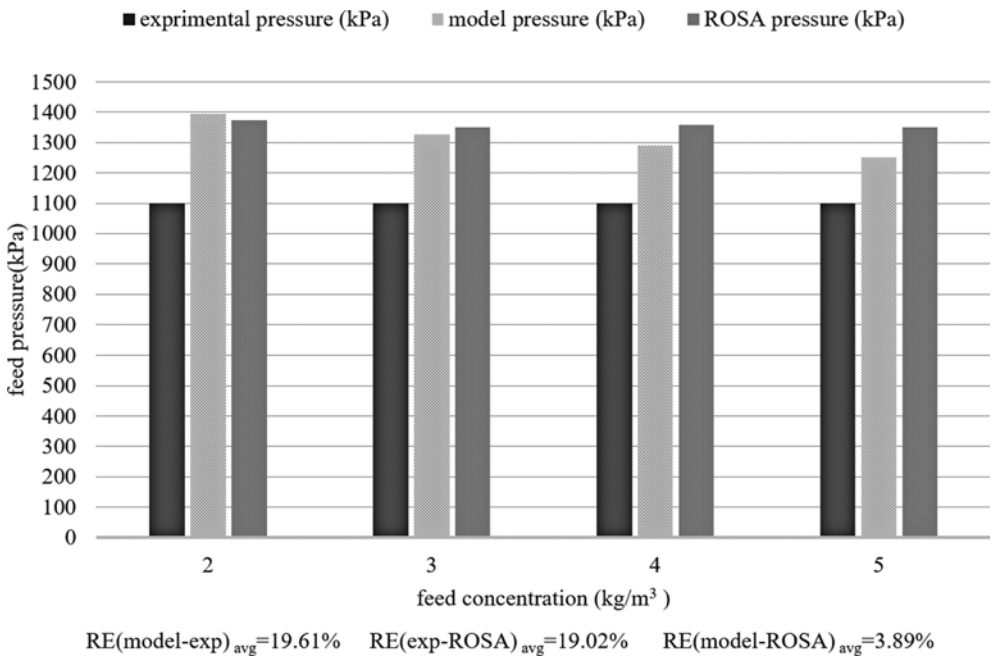

Fig. 8. Variation of Feed pressure in RO system with feed concentration (experimental pressure=1,100 kPa).

Table 5. Characteristics of case studies with two-pressure vessel and 5 elements in each pressure vessel

Number of elements in each pressure vessel	Element type	Number of pressure vessel	Temp (°C)	Recovery	$Q_{Permeate}$ (m^3/h)	Feed concentration (kg/m^3)
5	BW30-400	2	25	0.5	8	2

ference in results was expected. The ROSA software utilizes experimental equations that control Filmtec membranes, but in our simulation model the mathematical equations that control the RO process - based on the mass, material, and energy balance equations - are used. The equation that leads to significant differences is the one used for calculating the pressure drop in the membranes. The BW30-400 pure water permeability constant and the salt rejection used in the simulator model were obtained by laboratory data analysis (7.94e-9 (m/s·kPa) and 94.58-97.45%) that have a different quantity from the value set in ROSA (7.5e-9 (m/s·kPa) [8] and 97.76-99.25%).

It is observed in Tables 3 and 4 that by increasing the feed concentration, the permeate TDS estimated in both ROSA software and simulator model has a decreasing trend. It can also be justified using Eq. (5). The permeate TDS estimated by the proposed model is also closer (average ER: 1%) to the laboratory than estimated by the ROSA software. This is because the salt rejection in the ROSA software (97.76-99.25%) is different from our salt rejection in the laboratory (94.58-97.45%) and the proposed simulator model (94.63-97.47). Thus, for permeate TDS estimation the simulation model is accurate enough and well matched with the experimental results.

2-2. Multi-element Case

Since the experimental pilot has only one element in each pressure vessel, for the multi-pressure vessel and multi-element test cases, the comparisons were done between the simulation model and the ROSA software. For this purpose, a case study was simulated with several pressure vessels and several elements in each pressure vessel according to Table 5. The simulated results, including the required feed pressures, permeate flow rate and recovery of each element are found in Figs. 9-11.

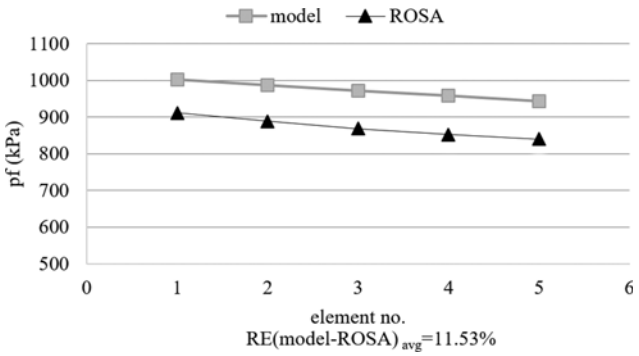

Fig. 9. Feed pressure for each element in RO system.

The calculated pressures are indicated in Fig. 9 where in each element by the simulation model and the ROSA software, shows that the pressure values in the first to fifth elements were 1,003, 988, 973, 958, and 943 in the proposed model and 912, 889, 869, 853 and 840 in the Rosa model and have decreasing trends in both. The average difference in the results was 100 kPa between the model and ROSA, which is according to the results reported by Altaee [2]. The highest and lowest RE was 12.26% and 9.9% in the fifth

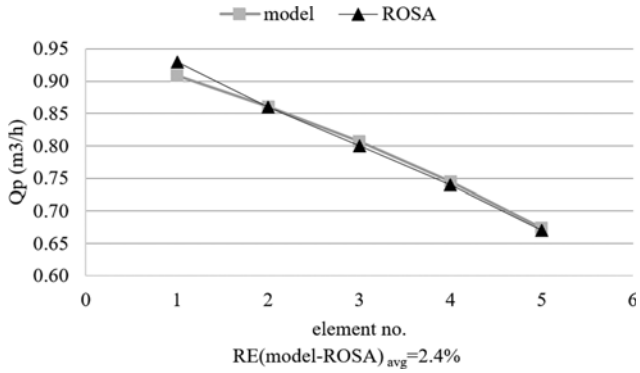

Fig. 10. Permeate flow rate for each element in RO system.

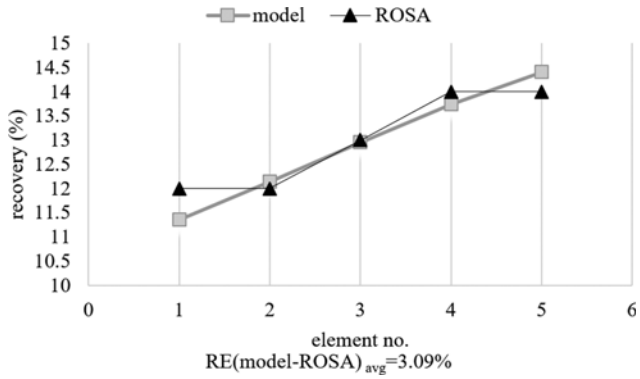

Fig. 11. Recovery for each element in RO system.

element and the first element, respectively; the average RE was 11.53%. The average pressure drop per element was 18 kPa and 15 kPa in ROSA and the simulation model, respectively, which are almost close to each other.

From Fig. 10, which shows the permeate flow rate in each element in the model and ROSA, it can be seen that the permeate flow rate value in the first to fifth elements was 0.93, 0.86, 0.8, 0.74, and 0.67 in ROSA and 0.88, 0.84, 0.8, 0.75, and 0.69 in the model where the results are very close [2]. The average RE was 2.4%, the highest RE was 5.3% in the first element, and the lowest RE was 0% in the third element.

In Fig. 11, which shows the recovery in each element in the model and ROSA, the recovery value in the first to fifth elements was 0.12, 0.12, 0.13, 0.14, and 0.14 in ROSA, and 0.11, 0.12, 0.13, 0.14, and 0.15 in the model where the results are very close [2]. The average RE was 3.09%.

Based on these obtained average RE values, it can be said that the pressure, the permeate flow rate, and the recovery calculated by the simulator model are (88.4%, 97.6%, 96.9%, respectively) accurately close to the calculated values by the ROSA software. Hence, the proposed algorithm functions well in the multi-elements RO systems. The calculated pressures by the model are slightly higher than the calculated pressures by ROSA. This could be due to laboratory conditions, measurement errors, and uncertainties and the simplifications applied to the simulation equations. Since the equations used in ROSA and the proposed simulation model are slightly different, this little difference in results was expected. The ROSA software utilizes experimental equations that control Filmtec membranes, but in our simulation model the mathematical equations that control the RO process are used. The equation that leads to significant differences is the one used for calculating the pressure drop in the membranes.

Based on two single element and multi-element cases result and RE value, the proposed simulation model functions well and is reliable. The calculated pressures by the simulation model are over 80% accurately close to the laboratory results and 96% accurately close to the results of the ROSA software.

CONCLUSION

A mathematical simulation model for the RO process, considering several series elements in each pressure vessel, was developed based on the mass, material, and energy balances considering the concentration polarization. Unlike other commercial software, the proposed model is open-source and since it is based on the mathematical equations of the RO process, it is capable of using all types of membranes manufactured by different companies. In the ROSA software, the percentage of the feed flow cannot be assigned to stage 2 and stage 3, and the feed flow first enters stage 1, and after treatment, the entire retentate from the first stage is considered as the feed water for the second stage. This issue happens between stage 2 and stage 3. However, in the proposed simulation model, given the three splitter points definition in the system, a certain percentage of the feed flow can be assigned to each stage. A percentage of the retentate from the first stage can also be removed from the system and a percentage of it can be added to each of the second and third stages. The former stream also happens between stage 2 and stage 3. Accordingly, in the ROSA software, the feed pressure of high-pressure pumps is related to the first stage, and the feed pressure of the second stage is the summation of retentate pressure from the first stage and the accelerator pump pressure. In the proposed simulation model, according to the three splitter point coefficients, the value of the high-pressure pumps is first determined in order to provide the pressure required for the first stage and according to the energy equation. Then, for the second and third stage, the amount of feed pressure is calculated by the energy equation. On the other hand, the retentate pressure considered as the feed for another stage is calculated concerning the energy equation, and the flow pressure prior to entering each stage is considered to be the minimum of the inflows to that stage. In case there is any need for a higher pressure, accelerator pumps are utilized.

An RO experimental pilot was constructed at the Hydraulic Lab of Shahid Chamran University of Ahwaz and used to validate the results of this simulation model. The performance of the laboratory pilot was evaluated and the results were discussed in detail.

The single element case was simulated using the proposed simulator model, and the results (including feed pressure, SEC, TDS permeate, and salt rejection) were compared with the ROSA software simulation and the experimental results. The multi-element case was simulated using the proposed simulator model, and the results (including feed pressure, permeate flow rate, and recovery in each element) were compared with ROSA.

Based on two single element and multi-element cases result and

RE value, it can be said that the comparison among the simulation model, the experiments, and the ROSA results indicates the reliability of the proposed simulation model. The calculated results by the simulation model are over 80% accurately close to the laboratory results and 96% accurately close to the ROSA software.

ACKNOWLEDGEMENTS

The authors would like to thank Ghadir Khuzestan Water Company and Khuzestan Water and Power Authority for their financial and technical support.

NOMENCLATURE

A : membrane surface area [m^2]
A_{eff} : effective surface area of membrane [m^2]
A_m : pure water permeability constant [m/s·kPa]
C : solution concentration [kg/m^3]
C_F : feed concentration [kg/m^3]
C_P : permeate concentration [kg/m^3]
C_R : retentate concentration [kg/m^3]
C_w : concentration on the feed side of membrane wall [kg/m^3]
d : membrane channel diameter [m]
Ds : solute diffusivity [m^2/s]
d_{sp} : spacer diameter [m]
i : stage counter
j : pressure vessel counter in stage
j_w : water flux [m^3/m^2·s]
k : mass transfer coefficient [m/s]
l_{ch} : length of the membrane channel [m]
M : molar concentration [mol/m^3]
n : van't Hoff factor
N_{ei} : number of the membrane element in pressure vessel of the i^{th} stage
Ni : number of membrane element in the i^{th} stage
N_{PVi} : number of pressure vessel in the i^{th} stage
P_{eff} : residual transmembrane pressure [kPa]
P_f : feed pressure [kPa]
P_p : permeate pressure [kPa]
Q_F : feed flow rate [m^3/s]
QF_{PV} : feed flow rate in the pressure vessel [m^3/s]
Q_{F1} : feed flow rate to the first stage [m^3/s]
Q_{F2} : feed flow rate to the second stage [m^3/s]
Q_{F3} : feed flow rate to the third stage [m^3/s]
Q_P : permeate flow rate [m^3/s]
QP_{PV} : permeate flow rate in the pressure vessel [m^3/s]
Q_R : retentate flow rate [m^3/s]
Q_{R1} : retentate flow rate from the first stage [m^3/s]
Q_{R2} : retentate flow rate from the second stage [m^3/s]
R : universal gases constant [8.314 m^3·Pa/mol·°K]
Re : Reynold's number
RE : relative error
rec1 : recovery in the first stage
rec2 : recovery in the second stage
rec3 : recovery in the third stage
Sc : schmidt number
St : spacer thickness [m]
T : temperature [°C]
T0 : reference temperature [25 °C]
TCF : temperature's correction factor
T_F : feed water temperature [°C]
V_{SP} : volume of the spacer [m^3]
V_T : total volume [m^3]
z : element counter in the Pressure vessel
μ : feed water viscosity [Pa·s]
α : fraction of the stream branching to the left from a split point
β : fraction of the stream branching to the right from a split point
γ : fraction of the stream branching straight forward from a split point
ΔP_f : pressure drop due to friction [kPa]
ΔP_{in} : pressure drop at inlet [kPa]
π : osmotic pressure [kPa]
π_p : osmotic pressure on the permeate side [kPa]
π_w : osmotic pressure on the feed side of membrane wall [kPa]
ρ : density [kg/m^3]
ε : Porosity

Subscripts
f : feed
F : feed split ratio
p : permeate
r : retentate
R1 : retentate split ratio for first module
R2 : retentate split ratio for second module

REFERENCES

1. H. Kotb, E. Amer and K. Ibrahim, *Desalination*, **357**, 246 (2015).
2. A. Altaee, *Desalination*, **291**, 101 (2012).
3. A. Villafafila and I. Mujtaba, *Desalination*, **155**, 1 (2003).
4. M. Barello, D. Manca, R. Patel and I. M. Mujtaba, *Comput. Chem. Eng.*, **83**, 139 (2015).
5. M. G. Marcovecchio, P. A. Aguirre and N. J. Scenna, *Desalination*, **184**, 259 (2005).
6. V. Geraldes, N. E. Pereira and M. Norberta de Pinho, *Ind. Eng. Chem. Res.*, **44**, 1897 (2005).
7. C. Guria, P. K. Bhattacharya and S. K. Gupta, *Comput. Chem. Eng.*, **29**, 1977 (2005).
8. Y.-Y. Lu, Y.-D. Hu, X.-L. Zhang, L.-Y. Wu and Q.-Z. Liu, *J. Membr. Sci.*, **287**, 219 (2007).
9. Y.-J. Choi, T.-M. Hwang, H. Oh, S.-H. Nam, S. Lee, J.-c. Jeon, S. J. Han and Y. Chung, *Desalination and Water Treatment*, **33**, 273 (2011).
10. Y. Du, L. Xie, Y. Wang, Y. Xu and S. Wang, *Ind. Eng. Chem. Res.*, **51**, 11764 (2012).
11. Y. Du, L. Xie, J. Liu, Y. Wang, Y. Xu and S. Wang, *Desalination*, **333**, 66 (2014).
12. Y. Du, L. Xie, Y. Liu, S. Zhang and Y. Xu, *Desalination*, **365**, 365 (2015).
13. E. R. Saavedra, A. G. Gotor, S. O. Pérez Báez, A. R. Martín, A. Ruiz-García and A. C. González, *Desalination and Water Treatment*, **51**, 4790 (2013).

14. E. Ruiz-Saavedra, A. Ruiz-García and A. Ramos-Martín, *Desalination and Water Treatment*, **55**, 2562 (2015).
15. J.-S. Choi and J.-T. Kim, *J. Ind. Eng. Chem.*, **21**, 261 (2015).
16. H. Kotb, E. Amer and K. Ibrahim, *Energy*, **103**, 127 (2016).
17. V. Haluch, E. F. Zanoelo and C. J. Hermes, *Chem. Eng. Res. Des.*, **122**, 243 (2017).
18. K. P. Chee, K. P. Wai, C. H. Koo and W. C. Chong, EDP Sciences, E3S Web of Conferences, 65, 05022 (2018).
19. M. Al-Obaidi, A. Alsarayreh, A. Al-Hroub, S. Alsadaie and I. M. Mujtaba, *Desalination*, **443**, 272 (2018).
20. C. Chen and H. Qin, *Processes*, **7**, 271 (2019).
21. O. P. Maure and S. Mungkasi, AIP Publishing LLC, AIP Conference Proceedings, 2202, 020043 (2019).
22. M. Li, *Chem. Eng. Res. Des.*, **148**, 440 (2019).
23. D. Gaublomme, L. Strubbe, M. Vanoppen, E. Torfs, S. Mortier, E. Cornelissen, B. De Gusseme, A. Verliefde and I. Nopens, *Desalination*, **490**, 114509 (2020).
24. J. Siegel, C. Wangmo, J. Cuhorka, A. Otoupalíková and M. Bittner, *Environ. Technol. Innovation*, **17**, 100584 (2020).
25. M. Ligaray, N. Kim, S. Park, J.-S. Park, J. Park, Y. Kim and K. H. Cho, *Chem. Eng. J.*, **395**, 125082 (2020).
26. T. M. Mansour, T. M. Ismail, K. Ramzy and M. Abd El-Salam, *Alexandria Eng. J.*, **59**, 3741 (2020).
27. DOW, FILMTEC Membranes, product information catalog, http://www.lenntech.com/feedback/feedback_uk.htm?ref_title=Filmtec/Filmtec-Reverse-Osmosis-Product-Catalog-L.pdf (2006).